Solid Freeform Fabrication 2017: Proceedings of the 28th Annual International Solid Freeform Fabrication Symposium – An Additive Manufacturing Conference
Reviewed Paper

ELECTROCHEMICAL ENHANCEMENT OF THE SURFACE MORPHOLOGY AND THE FATIGUE PERFORMANCE OF Ti-6Al-4V PARTS MANUFACTURED BY LASER BEAM MELTING

S. Bagehorn*, J. Wehr*, S. Nixon*, A. Balastrier*, T. Mertens**, H. J. Maier†

*Airbus, Airbus Group Innovations, 81366 München, Germany
** Airbus Operations GmbH, 28199 Bremen, Germany
†Institut für Werkstoffkunde (Materials Science), Leibniz Universität Hannover, 30823 Garbsen, Germany

Abstract

In the course of the industrialization of the Additive Manufacturing (AM) process of metallic components, the surface finish of the final parts is a key milestone. 'As-built' AM surfaces feature a high initial surface roughness (i.e. $R_a > 10$ µm), which often exceeds the specification for technical applications. In order to apply AM for highly stressed and cyclically loaded components, the as-built surface roughness needs to be reduced. Since conventional surface finishing processes as machining or blasting often show a limited applicability to complex shaped AM parts, an enhanced electrolytic polishing process was developed (3D SurFin®). Within the present study, Ti-6Al-4V AM plates and fatigue samples were produced in a powder bed laser beam system. The enhanced electrolytic polishing process led to a significant roughness decrease of approximately 84 % for a treatment time of 60 min. Also, a notable improvement of the fatigue performance of 174 % was achieved after a treatment time of 40 min in comparison to the as-built reference samples.

1. Introduction

The additive manufacturing (AM) technology is gaining increasing attention for actual industrial applications. Especially for the aerospace industry the processing of AM titanium components – and particularly the alloy Ti-6Al-4V (Ti64) – matters due to its beneficial corrosion resistance, its low density and the specific high strength [1]–[3]. Since the AM technology provides for a significant design freedom, topology optimized Ti64 components can be built by this layer-based manufacturing process leading to considerable savings of raw material, weight and therefore costs. This has triggered various studies, that report about the mechanical properties [4]–[8], the microstructural development [9]–[13], as well as various applications [14]–[16] of additively manufactured components.

Powder bed based laser beam melted (LBM) Ti64 parts are known to feature a high initial (‚as-built'[1]) surface roughness of typically more than $R_a = 10$ µm right after the manufacturing process [8], [17]–[19], which strongly depends on the orientation of the surfaces in the build chamber. This effect can be a limitation for the application of cyclically loaded or highly stressed components, as well as for further post-processing procedures applied on the surface. Therefore,

[1] The ‚as-built' condition later on refers to the morphological aspect of the initial rough surface regardless of the thermal history of a specimen.

the as-built surface roughness needs to be decreased. Although different build-up strategies during the manufacturing process can be employed to reduce surface roughness [20], [21], additional surface finishing processes are typically needed [22], [23]. As presented elsewhere, the focus of the surface finishing process is still on conventional machining procedures, which are known to increase the fatigue performance in comparison to the as-built samples [24]–[27]. Since the applicability of machining is limited for complex shaped parts as is the case for most AM components, new surface finishing procedures need to be developed. Due to their wet-chemical nature, electrochemical processes are very attractive for smoothening of complex shaped parts [19], [26]. Conventional electropolishing processes have already been studied on AM parts previously and showed promising results with respect to roughness reduction [19], [22], [28]. However, little is known about the enhancement of the fatigue performance of LBM Ti64 parts treated by these processes.

Figure 1 shows a schematic of the experimental setup for an electropolishing process consisting of two cathodic counter electrodes, a direct current supply and the component as the anode. The electrolyte filling level, as well as the temperature can be controlled. A circulation pump is used to create a suitable convection within the electrolyte.

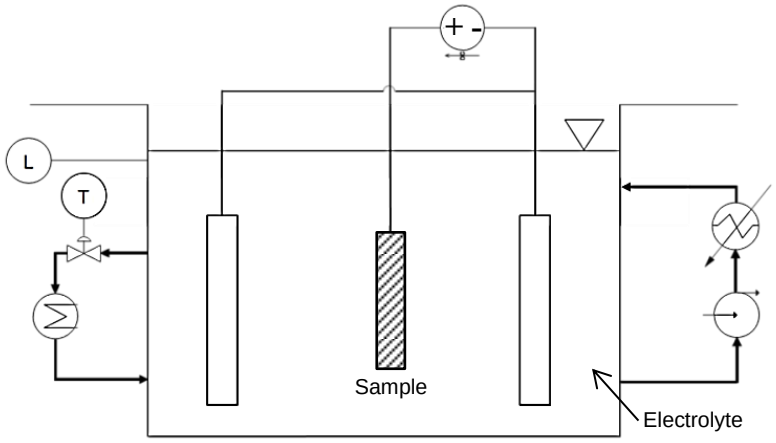

Figure 1: Process flow scheme of the experimental test setup for electrolytic polishing

For each application, the electrolyte needs to be chemically adapted to the alloy to be treated. Upon applying a direct current, an ion movement is initiated in the bath. During conventional electropolishing processes, roughness peaks are reduced when the flow conditions are such that transport through then near surface layer becomes the rate controlling step. However, the electrolytes used typically feature a high concentration of hazardous acids or alcohols [19], [22], [29], [30]. In addition, the treatment often comes along with substantial treatment times, or an undesirable high material removal leading to a considerable rounding of edges. Using alcohols in the electrolyte also induces the risk of explosion. Therefore, a new process based on the plasma electrolytic polishing process was developed, which will be referred to as the 3D SurFin® process in the following. The main differences to conventional electropolishing are the higher applied voltage range of approximately 200 – 400 V, the shorter treatment times and the use of REACh compliant electrolytes that are essentially based on water as reported elsewhere [26], [31]–[34].

Within this study, the influence of the treatment time of the 3D SurFin® process on the roughness of as-built LBM Ti64 plates was investigated. The focus was not only on the surface morphology but material removal and fatigue performance as well. Thus, fatigue samples were treated and compared with as-built samples to evaluate the effect of a smoothened surface on the fatigue performance.

2. Experimental

2.1 Sample manufacturing

The plates subsequently used for the characterization of the surface morphology were built at the Fraunhofer Institute ILT using a M270 laser beam system from EOS GmbH as described elsewhere [23]. All fatigue samples were manufactured by Liebherr Aerospace on a M290 laser beam system also from EOS GmbH. For all samples, TLS Technik GmbH supplied Ti-6Al-4V powder showing a spherical shape and an averaged particle size of 44 µm (D_{p50}). The nominal layer thickness during manufacturing was 30 µm. The plates were built with an energy density of 54.3 J/mm³, whereas an energy density of 55.6 J/mm³ was used for the build-up of the fatigue specimens. Prior to the removal from the build platform, all samples were stress relieved for 4 h at 540 °C under vacuum and cooled in an argon atmosphere. Afterwards, all samples were hot isostatically pressed (HIP) for 2 h at 810 °C and 2000 bar in an inert gas atmosphere to reduce the risk of fatigue failure by inner pores or other imperfections.

The characterization of the surface morphology prior and after the surface treatment was performed on plates with dimensions of 105 mm x 75 mm x 2 mm. They were built with an angle of 45° with respect to the build platform. According to [35]–[37], the surface facing the build platform at this angle shows the highest surface roughness without the use of support structures. Additionally, round fatigue samples were built vertically in z-direction under the same conditions in order to evaluate the effect of the surface treatment on the change in morphology and the corresponding fatigue behaviour. As described in [23], a build-up angle different to 90° would result in a significant deviation from the sample geometry, as well as the symmetry axis affecting the load transfer during subsequent testing. According to DIN EN 6072 [38], the sample geometry FCE type 25A with a diameter of 5.64 mm was chosen (K_t = 1.035, length: 80 mm). Figure 2 shows the corresponding drawing of the net shape geometry. One series was built with this exact geometry, whereas two other series were built with a minor additional offset of 0.3 mm within the diameter to cover the material removal during the surface finishing process. The threads (M16x1) were machined after the manufacturing, respectively after the surface finishing process.

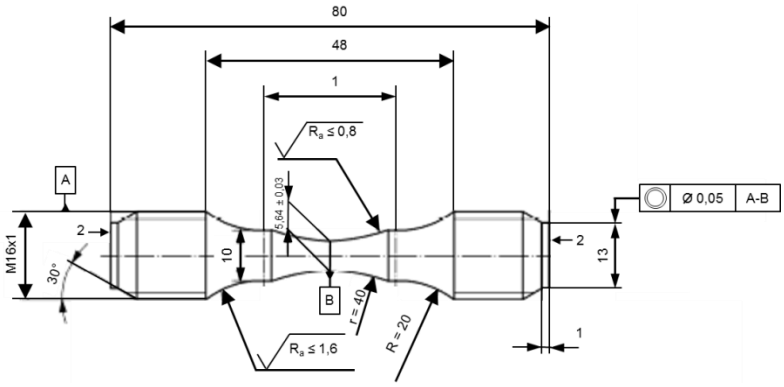

Figure 2: Round fatigue sample type FCE 25A (K_t = 1.035, length: 80 mm) according to DIN EN 6072 [38]

2.2 Surface finishing

Prior to surface smoothening, the plates and fatigue samples were cleaned by an alkaline cleaning detergent (P3 Almeco from Henkel) for about 15 min at 65 °C ± 3 °C. Afterwards, all samples were immersion rinsed in deionized water for 3 min at room temperature and subsequently dried at 60°C ± 2 °C in a circulating air oven.

The 3D SurFin® process was performed in a 200 l bath containing an electrolyte consisting of ammonium fluoride, sulphuric acid and a complex builder in accordance to [39]. The main ingredient of the electrolyte is deionized water with a mass percentage of > 80 wt.-%. As shown schematically in Figure 1, the electrolyte was continuously recycled by a pump and temperature was kept at 80 °C ± 3 °C. All samples were immersed vertically into the electrolyte with a set voltage of 300 – 350 V. Each of the three plates was treated sequentially to obtain a total treatment time of 2 min, 5 min, 10 min, 20 min, 40 min and 60 min. The two sets of fatigue specimens were separately smoothened for 20 min, respectively 40 min. After the treatment, all samples were immersion rinsed and dried according to the procedure after alkaline cleaning.

2.3 Material characterization

For the characterization of the surface condition prior to and after the treatment, the surface roughness was analysed according to DIN EN 4287 [40]. The roughness values R_a, R_z, R_t and R_v were measured using a Hommel Etamic Waveline profilometer T8000 with an accuracy of 0.002 µm. All roughness values were determined three times in longitudinal direction on each side of the three plates.

A scanning electron microscope (SEM) JSM 6320F from Jeol was employed to obtain high resolution micrographs. Each sample was sputtered with a platinum layer with a thickness of 4 nm prior to the SEM investigations. Additionally, an Auriga SEM from Zeiss equipped with a X-Max^N 50 detector from Oxford Instruments was used to determine the chemical composition of the surface by energy dispersive X-ray spectroscopy (EDX). For titanium surfaces, the penetration depth was calculated to be 1.7 µm for the characterization of the chemical composition by EDX.

The material removal was determined by differential weighting on a balance from Kern with a accuracy of ± 0.01 g.

2.4 Fatigue testing

The fatigue samples were tested on two machines from Rumul. The samples with the as-built surface condition were tested on a Mikrotron test rig, whereas the electrolytically polished samples were tested on a Fractronic test rig. Both machines were equipped with a 24 kN load cell and calibrated prior to testing. The accuracy of the stress amplitudes were found to be within ± 1 % of the nominal values for both machines. The tests were performed at ambient temperature, a frequency of approximately 110 Hz and with an axial fatigue stress ratio of $R = 0.1$ at constant maximum stress levels. The fatigue limit was set to 3×10^7 cycles, which will be referred to as 'run-out' in the following.

The fracture surfaces of broken fatigue specimens were analysed using the JSM 6320F SEM for a detailed investigation of fracture morphology and crack initiation sites.

3. Results

3.1 Surface morphology

As described in [23] the as-built surfaces of additively manufactured Ti64 parts show a high initial surface roughness resulting from partially melted particles on top of the surface. This is demonstrated in Figure 3, which shows an irregular distribution of the particles leading to locally varying surface conditions. Moreover, it demonstrates a significant surface waviness, which can be classified as primary roughness caused by the melt pool during the manufacturing process [25]. The surface shown in Figure 3 also features deep roughness furrows, which are hardly visible due to the particles on top of the surface contour.

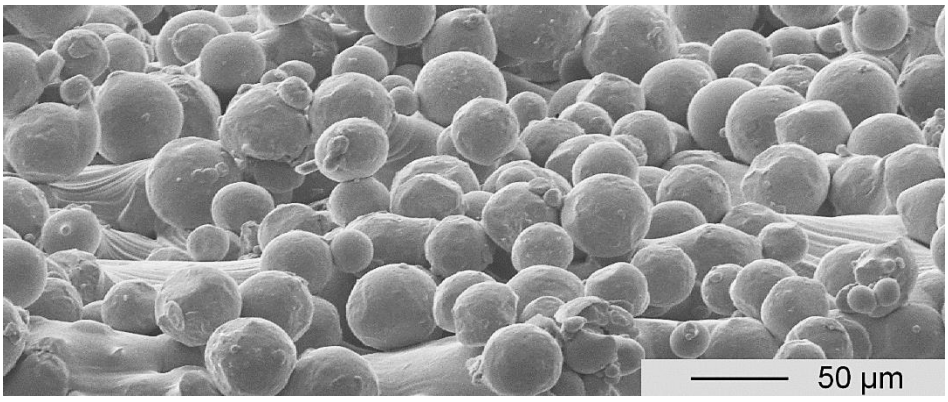

Figure 3: SEM micrograph of an as-built surface revealing partially melted particles responsible for the high initial surface roughness

The averaged roughness values measured on the so called 'downskin' surface, which is facing the build plate, as well as on the 'upskin' surface on the opposite side are pointed out in Table 1 for the three plates. The R_a values show a difference of approximately 11 % between both sides,

whereas the downskin face features higher roughness values in the as-built state. The standard guidelines for most technical applications often call for much lower roughness values, and the results in Table 1 demonstrate that the as-built surfaces by far exceed the specifications.

Table 1: Surface roughness values of the upskin and downskin side averaged out of three plates prior and after surface finishing (after 60 min)

	R_a, µm	R_z, µm	R_t, µm	R_v, µm
Upskin as-built surface	15.6 ± 1.3	118.9 ± 9.3	145.9 ± 20.0	51.2 ± 3.2
Downskin as-built surface	17.6 ± 0.7	131.5 ± 7.8	156.3 ± 12.6	56.3 ± 4.0
Upskin surface after 3D SurFin®	2.8 ± 0.5	19.4 ± 5.1	26.9 ± 9.1	8.9 ± 1.8
Downskin surface after 3D SurFin®	2.6 ± 0.3	17.0 ± 2.9	23.1 ± 6.1	8.0 ± 1.2

Figure 4a) demonstrates the roughness decrease of the R_a value of the upskin, as well as of the downskin surface after different surface finishing treatment times. The averaged results for both sides of the plate out of all three plates were calculated. The values after 60 min are also listed in Table 1 for both sides. Averaged over all three plates, the roughness could be reduced by about 84 % for a treatment time of 60 min. In addition, the initially different values of both sides became similar during the process. Although most of the change in surface roughness occurred in the first 40 min of the process, the material removal was still ongoing during the final 20 min (see Figure 4b)). Within that time, a weight loss of approximately 7.27 g ± 0.01 g resulted. In total, the plates lost an average weight of approximately 20.87 g ± 0.01 g. According to Figure 4b), the material removal follows a nearly linear trend over time despite the change in surface morphology.

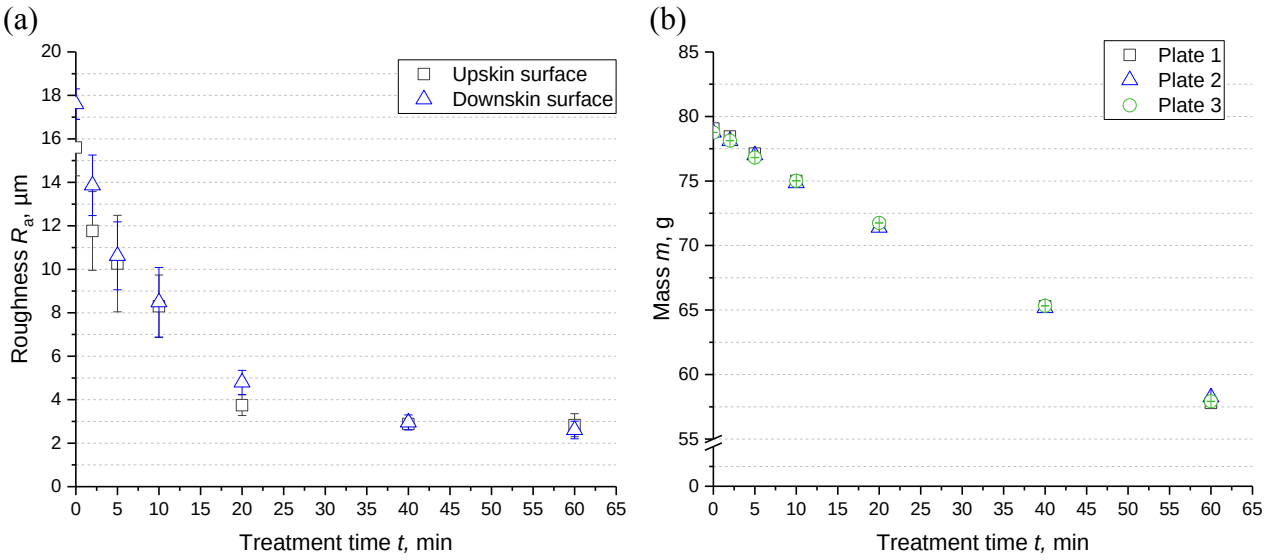

Figure 4: (a) averaged results for the roughness values R_a of the upskin and the downskin surfaces of all three plates after different treatment times for the 3D SurFin® process; (b) corresponding weight decrease

Figure 5 shows the corresponding SEM micrographs after each treatment time from 2 min to 60 min. After 2 min, Figure 5a) already demonstrates an obvious attack on the single particles, as well as on additional roughness features. Higher magnifications of this surface revealed an additional compact layer around the particles, as well as on top of the surface contour, which was partially dissolved. Applying a treatment time of 5 min (Figure 5b)), a significant roughness reduction was visible and most of the partially melted particles could be removed. To some extent the compact layer was still visible after 5 min, but fully vanished after a total treatment time of 10 min. As shown in Figure 5c), all particles could be removed after 10 min. and the microstructure of the substrate became visible. Although the SEM micrographs in Figure 5d)-f) indicate no further substantial change in morphological structure, isolated remaining roughness valleys as exemplary shown in Figure 5d). Further material removal could decrease the furrows and led to a more homogeneous surface morphology (Figure 5f)).

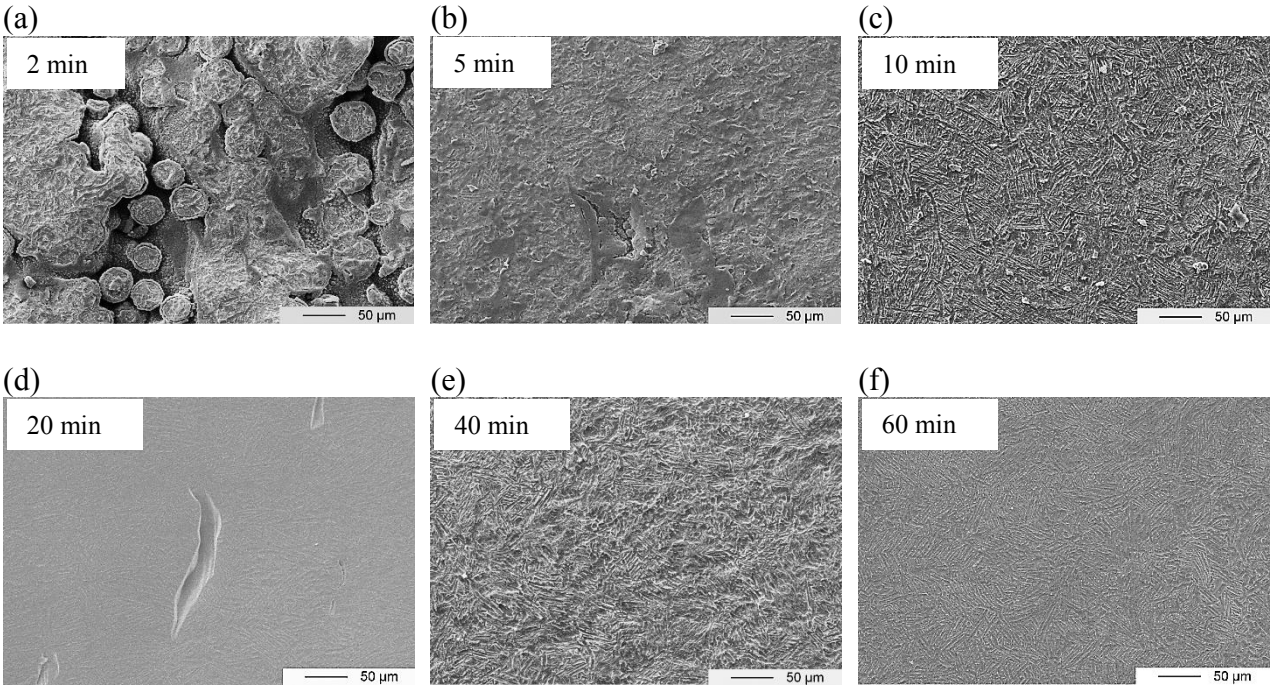

Figure 5: SEM micrographs of LBM Ti64 surfaces after different treatment times: (a) 2 min, (b) 5 min, (c) 10 min, (d) 20 min, (e) 40 min, (f) 60 min

A SEM micrograph of the LBM Ti64 surface after a treatment time of 2 min is shown at a higher magnification in Figure 6a). It details the initial powder particles, which were partially removed and coincidently encased with a material, which was different from bulk alloy. The thickness of this layer was approximately 3 - 6 µm. The corresponding EDX analyses are displayed in Figure 6b) and (c). As seen in Figure 6c), the central surface of the larger particle mainly consists of the elements expected for the bulk material Ti64 accompanied by some minor decontamination from the electrolyte (fluoride, sodium) and the environment (carbon). Figure 6b) reveals the element distribution of the layer formed on top of the particles. Besides typical contaminations (carbon, oxygen), this layer mainly consists of a titanium-fluoride compound and additional elements,

which can be found in the electrolyte. Additional EDX analyses have been conducted in more areas on this sample, which all confirmed this trend.

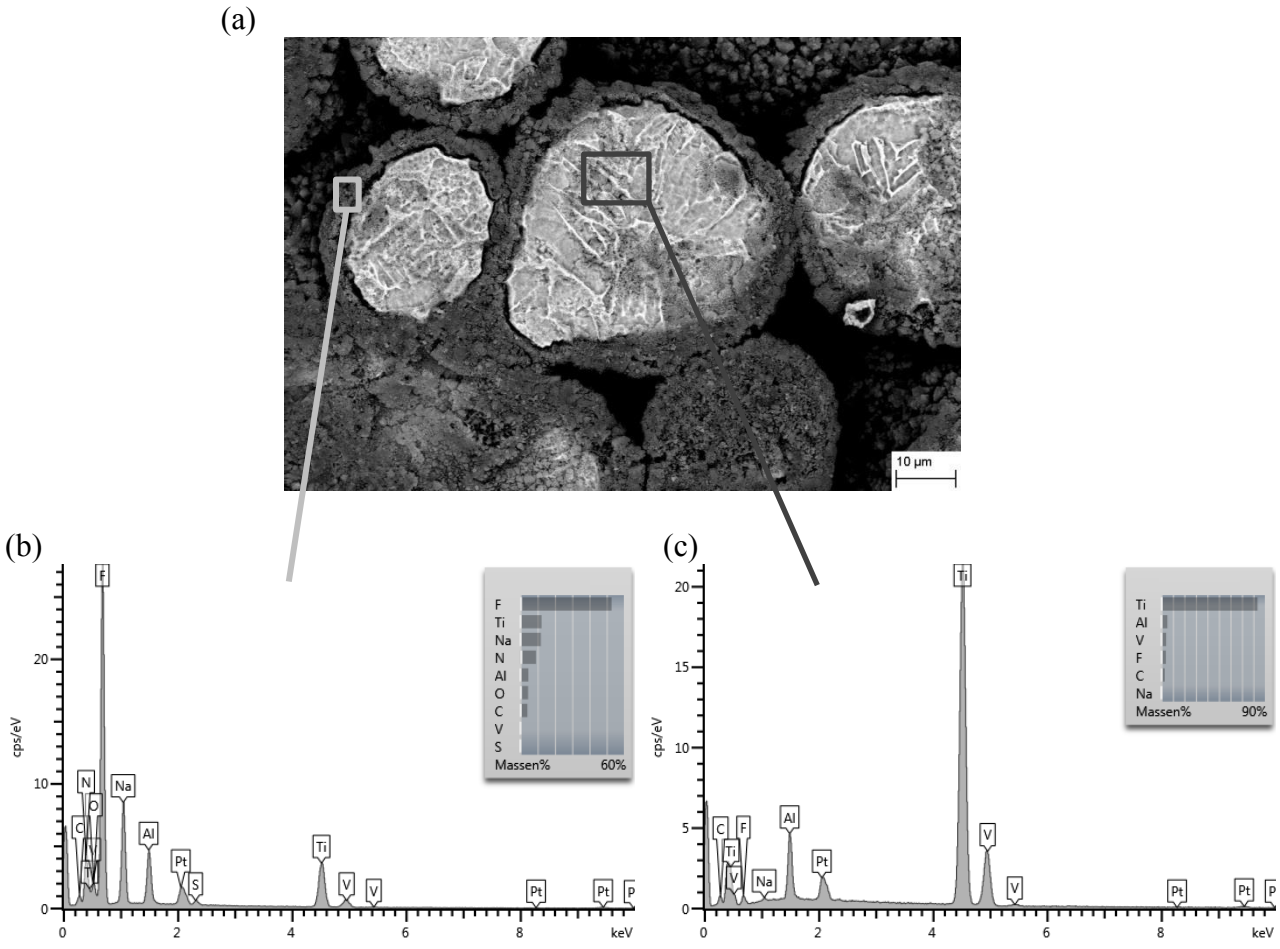

Figure 6: (a) Backscatter SEM micrograph of the LBM Ti64 surface after a treatment time of 2 min; (b) EDX analysis of the surface layer formed on top of the roughness particles; (c) EDX analysis of a particle from the bulk material

3.2 Fatigue results

The results of the fatigue specimens with as-built and after 3D SurFin® with 20 min and 40 min treatment time are displayed in Figure 7. The as-built test series demonstrated a substantially lower fatigue performance in comparison to samples with smoother surfaces. Two 'run-outs' were manually stopped after 3 x 10^7 cycles at 250 MPa and 350 MPa. A typical crack initiation site for this test series is shown in Figure 8 for a sample that failed after 4.1 x 10^4 cycles at a maximum stress level of 500 MPa.

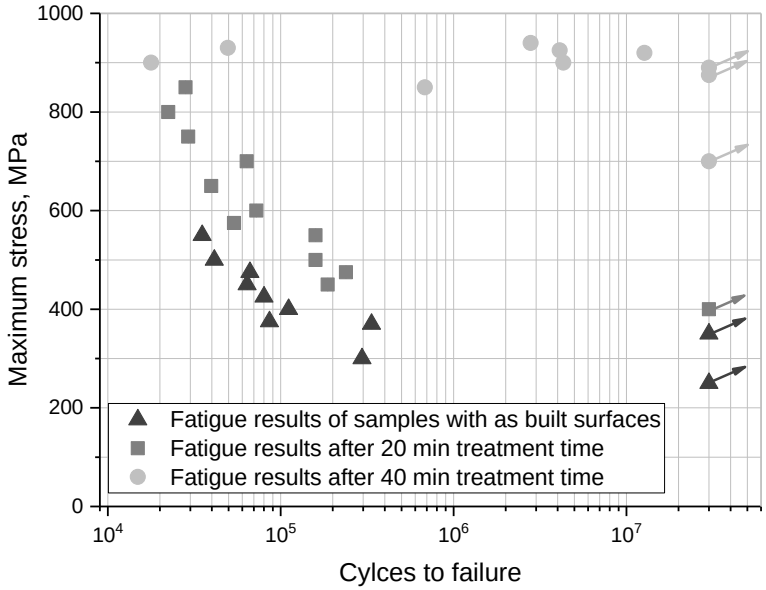

Figure 7: Comparison of the fatigue results of samples with as-built surface and with surfaces resulting from the 3D SurFin® process after treatment times of 20 min and 40 min

In Figure 8a) the crack initiation site is marked by a white rectangle. The higher magnification in Figure 8b) reveals a nucleation from a roughness valley at the outer surface contour. This type of crack initiation was typical for all as-built samples.

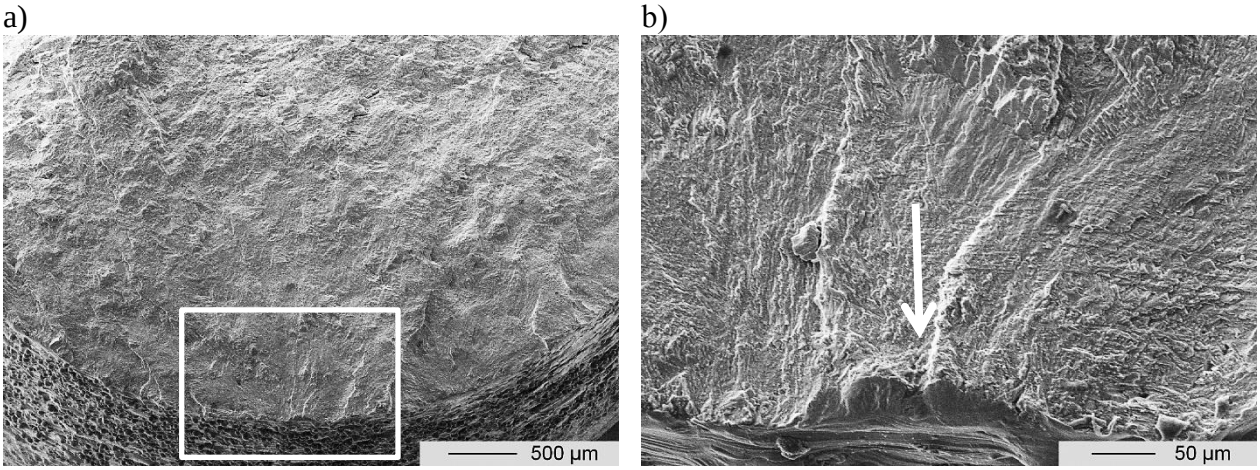

Figure 8: SEM micrograph of the fracture surfaces of a sample with an as-built surface condition that failed at a maximum stress of 500 MPa: (a) overview of the fractured surface, (b) detailed micrograph at the crack initiation site

In order to investigate the influence of the surface finishing process on the fatigue behaviour, two additional test series with a treatment time of 20 min and 40 min were tested as seen in Figure 7. For both series, the fatigue life improved substantially compared to the as-built samples. A 'run-out' was obtained after 3 x 10^7 cycles at 400 MPa for the fatigue specimens smoothened after a treatment time of 20 min. Figure 9a) demonstrates the most prevalent crack initiation site using the case of a sample broken after 1.6 x 10^5 cycles at a maximum stress level of 500 MPa. The

nucleation site is again marked with a white rectangle. The higher magnification in Figure 9b) reveals nucleation from a roughness valley at the outer surface contour.

The samples that were treated for 40 min using the 3D SurFin® process, achieved a more significant improvement of the fatigue performance compared to the treatment time of 20 min. In this case, three 'run-outs' were obtained at a maximum stress level of 700 MPa, 875 MPa and 890 MPa after 3 x 10^7 cycles. Taking the averaged maximum stress values of the 'run-outs' of the as-built and the 40 min polished test series into account, an increased fatigue performance of approximately 174 % can be calculated compared to the as-built condition.

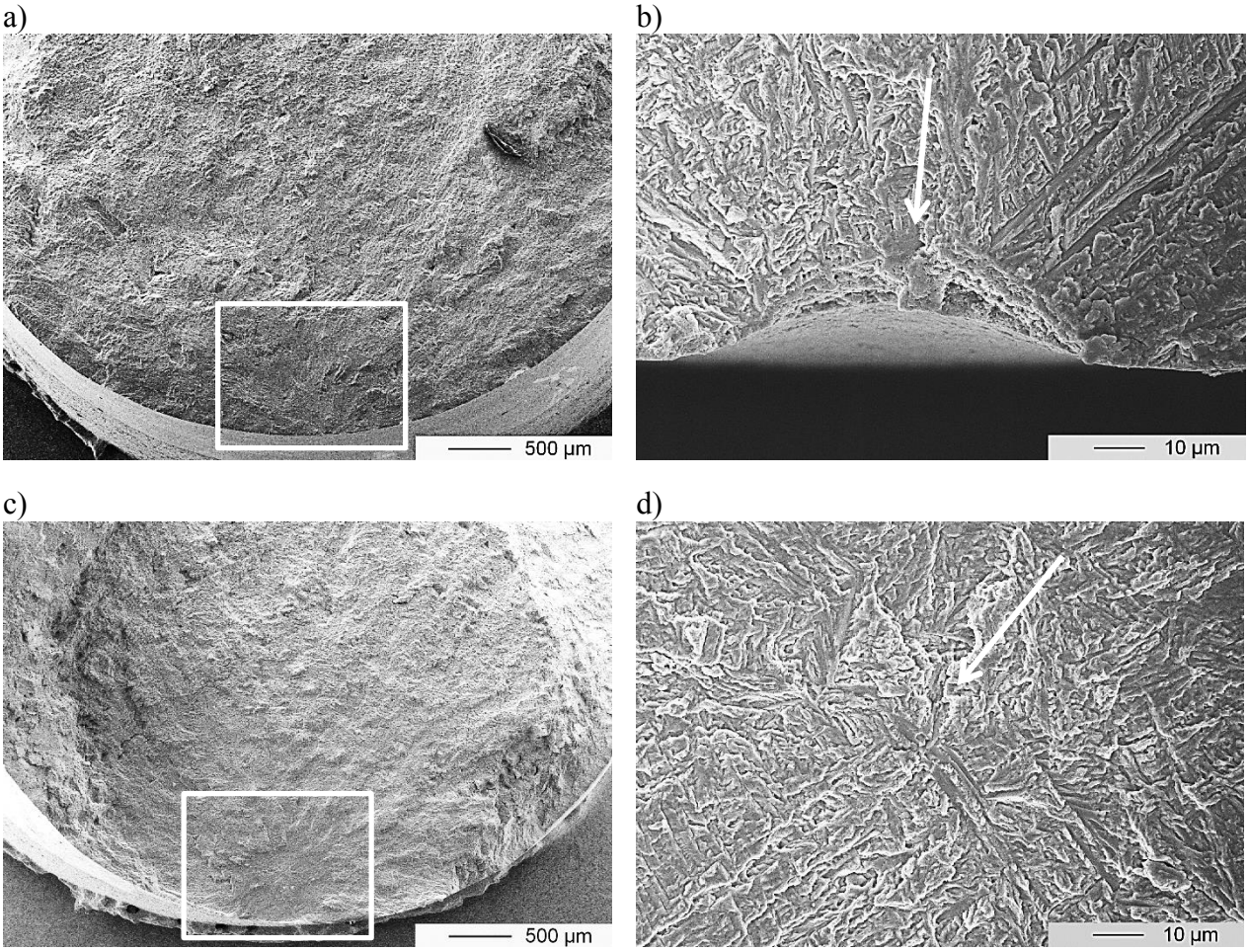

Figure 9: SEM micrograph of fracture surfaces of broken samples after the 3D SurFin® process with a treatment time of 20 min ((a), (b)) and 40 min ((c), (d))

Figure 9c) indicates the crack nucleation site of a sample treated for 40 min, which failed after 4.1 x 10^6 cycles at a stress level of 925 MPa. Again, the crack nucleation is marked by a white rectangle. As seen at the higher magnification in Figure 9d), the crack nucleated within the bulk material. This failure mode was prevalent for this entire test series.

4. Discussion

As reported elsewhere [8], [15], [19], the LBM Ti64 parts feature a high initial roughness resulting from the manufacturing process. The morphological difference between the upskin and the downskin surface of the plates built under an angle of 45° can be attributed to the so called staircase effect as described in [35], [36]. Consequently, as-built surfaces reveal significant roughness valleys and therefore notch effects, which cause a considerably lower fatigue performance as expected from previous reports [6], [17], [18]. The enhanced electrolytic polishing process (3D SurFin®) significantly reduced the surface roughness. Although different roughness values R_a were initially measured for the upskin and the downskin side, the final values of both sides converged to an average roughness of $R_a = 2.7\ \mu m \pm 0.5\ \mu m$ after a treatment time of approximately 40 min. As demonstrated by the SEM micrographs, most of the features being responsible for the high roughness could be removed after approximately 10 – 20 min with the 3D SurFin® process. The material loss tended to show a linear decrease over time, i.e. the behaviour is similar to conventional electropolishing processes [19] in this respect.

As presented in Figure 6a) - b), a 3 - 6 µm thick layer was built-up on top of the surface during the first 2 min. The layer mainly consists of a titanium-fluoride compound and a few additional elements, which are present in the electrolyte as well. This layer could also be found on the surfaces between and underneath the former powder particles. As it contains a considerable amount of titanium, the layer might result from the first dissolved material agglomerating or complexing close to surface areas with low electrolyte replacement due to less convection. The layer could be removed completely after a treatment time of approximately 10 min.

Clearly, the as-built surfaces cause a substantial decrease in fatigue performance in comparison to conventional cast or wrought parts [2], [3]. By contrast, the smoothened fatigue samples demonstrated increased fatigue life, especially the specimens treated for 40 min. This can be attributed to the change in surface morphology as the SEM micrograph in Figure 5e) indicates that no roughness valleys and no initial powder particles remained at the surface after this treatment. This even led to an improvement of the performance compared to milled (hot isostatically pressed) LBM Ti64 samples [23], [25]. As indicated in Figure 9c), the broken specimens typically failed due to crack initiation in the bulk material but no longer by cracks formed at the surface. The slight scatter within the results, which differ from the expected shape of the fatigue curve, might be referred to the fact that the applied stress amplitudes are close to the plastic deformation regime for hot isostatically pressed LBM Ti64 [7].

By comparison, the roughness decrease after a treatment time of 20 min showed a substantially smaller fatigue improvement of approximately 33 %. From Figure 5d), it becomes apparent that particles were no longer present on the surface, but some considerable roughness valleys remained due to unsufficient material removal. Therefore, a treatment time of at least 40 min is needed in this process to obtain a balanced relation between material removal and increase in fatigue performance.

This effect leads to the assumption that there is no direct correlation between the fatigue performance and the individual roughness values. This effect was previously shown in [23]. The roughness valleys in Figure 5d) might be missed by tactile roughness measurements leading to

more optimistic results. Alternative surface characterization methods such as imaging techniques or dye penetrant inspection could be used to assure the absence of surface defects.

5. Conclusion

Additively manufactured metallic components feature a high initial surface roughness right after the manufacturing process, which needs to be decreased for further post-processing as well as for the application in cyclically loaded components. In the present study an enhanced electrolytic polishing process (3D SurFin®) was applied on LBM Ti64 plates and fatigue specimens in order to evaluate its efficiency in terms of roughness reduction, as well as improvement of fatigue performance. Based on the results, the following main conclusions can be drawn:

- A high initial surface roughness with an averaged R_a of 16.6 µm ± 1.0 µm was measured on the LBM Ti64 plates for the as-built surface condition. This is a result of partially melted powder particles, as well as a high surface waviness caused by the manufacturing process.
- The notch sensitive LBM Ti64 samples with the as-built surface condition displayed a deteriorated fatigue performance with two run-outs at 250 MPa and 350 MPa after 3 x 10^7 cycles.
- The application of the 3D SurFin® process could reduce the initial roughness to a final averaged value of R_a = 2.7 µm ± 0.4 µm within a treatment time of 60 min.
- Treating fatigue samples by the enhanced electrolytic polishing process, the fatigue performance could considerably be increased. For a treatment time of 40 min, the technical endurance limit was around 820 MPa after 3 x 10^7 cycles, which is similar to the value obtained for hot isostatically pressed, milled LBM Ti64 fatigue samples.
- A treatment time of 20 min resulted in a lower improvement which could be attributed to an insufficient material removal leaving occasional roughness valleys, which could still cause a crack initiation from the outer surface contour.

Acknowledgements

The present study was supported by the German aeronautic research program (LuFo) within the framework of the project GenFLY. The authors thank the project sponsor Airbus, as well as the corresponding project partners Liebherr Aerospace and Fraunhofer ILT. The corresponding author also thanks Norbert Schupp, Max Kolb, Vitus Holzinger, Christian Plander and Freerk Syassen for their support.

References

[1] Lütjering G, Williams JC. Titanium. 2nd ed. Germany: Springer; 2007.
[2] Campbell FC. Manufacturing technology for aerospace structural materials. 1st ed. Great Britain: Elsevier Ltd.; 2006.
[3] Boyer R, Collings EW, WelschG. Materials Properties Handbook: Titanium Alloys. 2nd ed. USA: ASM International; 1998.
[4] Leuders S, Thöne M, Riemer A, Niendorf T, Tröster T, Richard HA, Maier, HJ. On the

mechanical behaviour of titanium alloy TiAl6V4 manufactured by selective laser melting: Fatigue resistance and crack growth performance. Int. J. Fatigue 2013; 48: 300–307.
[5] Kasperovich G, Hausmann J. Improvement of fatigue resistance and ductility of TiAl6V4 processed by selective laser melting. J. Mater. Process. Technol. 2015; 220: 202–214.
[6] Wycisk E, Solbach A, Siddique S, Herzog D, Walther F, Emmelmann C. Effects of Defects in Laser Additive Manufactured Ti-6Al-4V on Fatigue Properties. Phys. Procedia 2014; 56: 371–378.
[7] Lewandowski J, Seifi M. Metal Additive Manufacturing: A Review of Mechanical Properties. Annu. Rev. Mater. Res. 2016; 46(1): 151–186.
[8] Simonelli M, Tse YY, Tuck C. Effect of the build orientation on the mechanical properties and fracture modes of SLM Ti–6Al–4V. Mater. Sci. Eng. A 2014; 616: 1–11.
[9] Brandl E, Greitemeier D. Microstructure of additive layer manufactured Ti–6Al–4V after exceptional post heat treatments. Mater. Lett. 2012; 81: 84–87.
[10] Song B, Dong S, Zhang B, Liao H, Coddet C. Effects of processing parameters on microstructure and mechanical property of selective laser melted Ti6Al4V. Mater. Des. 2012; 35: 120–125.
[11] Qiu C, Adkins NJE, Attallah MM. Microstructure and tensile properties of selectively laser-melted and of HIPed laser-melted Ti–6Al–4V. Mater. Sci. Eng. A 2013; 578: 230–239.
[12] Antonysamy AA. Microstructure, Texture and Mechanical Property Evolution during Additive Manufacturing of Ti6Al4V Alloy for Aerospace Applications. England: The University of Manchester 2012.
[13] Thijs L, Verhaeghe F, Craeghs T, Van Humbeeck J, Kruth JP. A study of the microstructural evolution during selective laser melting of Ti–6Al–4V. Acta Mater. 2010; 58 (9): 3303–3312.
[14] Wang Y, Shen Y, Wang Z, Yang J, Liu N, Huang W. Development of highly porous titanium scaffolds by selective laser melting. Mater. Lett. 2010; 64(6): 674–676.
[15] Vandenbroucke B, Kruth J. Selective laser melting of biocompatible metals for rapid manufacturing of medical parts. Rapid Prototyp. J. 2007; 13(4): 196–203.
[16] Uriondo A, Esperon-Miguez E, Perinpanayagam S. The present and future of additive manufacturing in the aerospace sector: A review of important aspects. Proc. Inst. Mech. Eng. Part G J. Aerosp. Eng. 2015; 229(11): 2132–2147.
[17] Edwards P, Ramulu M. Fatigue performance evaluation of selective laser melted Ti–6Al–4V. Mater. Sci. Eng. A. 2014; 598: 327–337.
[18] Greitemeier D, Dalle Donne C, Syassen F, Eufinger J, Melz T. Effect of surface roughness on fatigue performance of additive manufactured Ti–6Al–4V. Mater. Sci. Technol. 2016; 32(7): 629–634.
[19] Urlea V, Brailovski V. Electropolishing and electropolishing-related allowances for powder bed selectively laser-melted Ti-6Al-4V alloy components. J. Mater. Process. Technol. 2017; 242: 1–11.
[20] Gebhardt A, Hötter JS, Ziebura D. Impact of SLM build parameters on the surface quality. RTejournal - Forum für Rapid Technol. 2014; 2014(11).
[21] Wang Z, Chen G, Guan K, Peng C, Zeng X. Effects of parameters on surface roughness of samples by selective laser melting. In: Proceedings of ICALEO 2009; 1902.
[22] Longhitano G, Larosa M, Munhoz A. Surface Finishes for Ti-6Al-4V Alloy Produced by Direct Metal Laser Sintering. Mater. Res. 2015; 18(4): 838–842.
[23] Bagehorn S, Wehr J, Maier HJ. Application of mechanical surface finishing processes for

roughness reduction and fatigue improvement of additively manufactured Ti-6Al-4V parts. Int. J. Fatigue 2017; 102: 135–142.
[24] Rafi H, Starr T, Stucker B. A comparison of the tensile, fatigue, and fracture behavior of Ti-6Al-4V and 15-5 PH stainless steel parts made by selective laser melting. Int. J. Adv. Manuf. Technol. 2013; 69(5): 1299–1309.
[25] Greitemeier D. Untersuchung der Einflussparameter auf die mechanischen Eigenschaften von additiv gefertigtem TiAl6V4. Darmstadt: Springer; 2016.
[26] Bagehorns S, Mertens T, Seack O, Maier HJ. Reduction of the surface roughness of additively manufactured metallic parts by enhanced electrolytic smoothening. In: Proceedings of Rapid.Tech 2016 Conference, June 2016 14–16; Erfurt, Germany.
[27] Zhao X, Li S, Zhang M, Liu Y, Sercombe T, Wang S, Hao Y, Yang R, Murr LE. Comparison of the microstructures and mechanical properties of Ti–6Al–4V fabricated by selective laser melting and electron beam melting. Mater. Des. 2016; 95: 21–31.
[28] Yang L, Gu H, Lassell A. Surface treatment of Ti6Al4V parts made by powder bed fusion additive manufacturing processes using electropolishing. In: Proceedings of the 25th Solid Freeform Fabrication Symposium, August 2014 10-12; Austin, USA.
[29] Mathieu JB, Mathieu HJ, Landolt D. Electropolishing of Titanium in Perchloric Acid-Acetic Acid Solution. J. Electrochem. Soc. 1978; 125(7): 1039–1043.
[30] ASTM E1558-09. Standard Guide for Electrolytic Polishing of Metallographic Specimens. 2014
[31] Mayorov A, Berkovich A. Plasma-electrolytic polishing of metals products. US20100200424 A1, 2010.
[32] Nestler K, Adamitzki W, Unger M, Faust W, Meyer W. Plasma Polishing of Metallic Surfaces - Effects and Models. In: Proceedings of International Symposium on Electrochemical Machining Technology, October 2006 26-27; Dresden, Germany.
[33] Nestler K, Böttger-Hiller F, Adamitzki W, Glowa G, Zeidler H, Schubert A. Plasma Electrolytic Polishing - an Overview of Applied Technologies and Current Challanges to Extend the Polishable Material Range. Procedia CIRP 2016; 42: 503–507.
[34] Kißling S. Chemische und elektrochemische Methoden zur Oberflächenbearbeitung von galvanogeformten Nickel-Mikrostrukturen. Germany: Karlsruher Institute of Technology, 2010.
[35] Sehrt JT. Möglichkeiten und Grenzen bei der generativen Herstellung metallischer Bauteile durch das Strahlschmelzverfahren. Germany: Universität Duisburg-Essen, 2010.
[36] Pyka G, Kerckhofs G, Papantoniou I, Speirs M, Schrooten J, Wevers M. Surface Roughness and Morphology Customization of Additive Manufactured Open Porous Ti6Al4V Structures. Materials 2013; 6(10): 4737–4757.
[37] Abele E, Kniepkamp M. Analysis and optimisation of vertical surface roughness in micro selective laser melting. Surf. Topogr. Metrol. Prop. 2015; 3(3): 34007.
[38] DIN EN 6072. Luft- und Raumfahrt – Metallische Werkstoffe – Prüfverfahren - Ermüdungstest mit konstanter Amplitude. 2010.
[39] Bagehorn S, Mertens T, Syassen F. Electrolyte and process for the electrolytic polishing of a metallic substrate. EP 3 109 348 A1, 2016.
[40] DIN EN ISO 4287. Geometrische Produktspezifikation (GPS) – Oberflächenbeschaffenheit: Tastschnittverfahren. 2009.